Supplement of Geosci. Model Dev., 18, 3781–3798, 2025
https://doi.org/10.5194/gmd-18-3781-2025-supplement

Geoscientific Model Development
Open Access

Supplement of

The sensitivity of aerosol data assimilation to vertical profiles: case study of dust storm assimilation with LOTOS-EUROS v2.2

Mijie Pang et al.

Correspondence to: Jianbing Jin (jianbing.jin@nuist.edu.cn) and Wei Han (hanwei@cma.gov.cn)

1. AOD assimilation

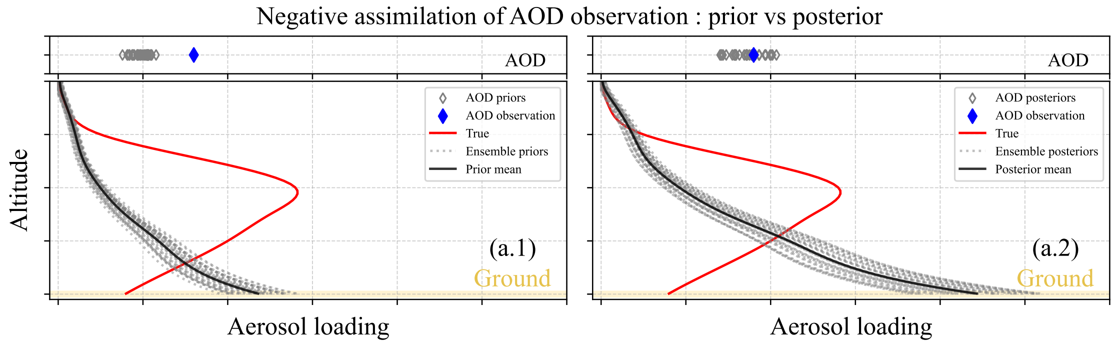

Fig. S1. Another schematic diagram of the sensitivity of AOD data assimilation to aerosol vertical structure. Assimilation of AOD observation under negative condition with AOD priors (gray hollow diamond), AOD observation (blue solid diamond) in upper box and true profile (red line), ensemble priors (gray dash line), prior mean (black line), ground observation (blue star) in lower box (**a.1**). Figure on the right are for the posteriors (**a.2**).

2. CALIOP dust classification

The polarization lidar–photometer networking (POLIPHON) technology was applied to classify dust and non-dust aerosol components and to estimate the fine and coarse dust contributions to the overall backscatter and extinction coefficients and particle mass concentration [1, 2]. The method is solely based on the use of characteristic depolarization ratios for fine dust, coarse dust, and non-dust aerosol.

The dust backscatter coefficient β_d is calculated by:

$$\beta_d = \begin{cases} \beta_p & \delta_p \geq \delta_d \\ \beta_p \frac{(\delta_p - \delta_{nd})(1+\delta_d)}{(\delta_d - \delta_{nd})(1+\delta_p)} & \delta_{nd} < \delta_p < \delta_d \\ 0 & \delta \leq \delta_{nd} \end{cases} \tag{S1}$$

where δ_p, δ_d and δ_{nd} are the depolarization ratio of total particle, dust (fine+coarse) and non-dust, respectively. β_p is the particle backscatter coefficient. For reference, δ_d is set to be 0.31 under the wavelength of 532 nm. And δ_{nd} is assumed to be 0.05. From this equation we can tell that δ_p greater than δ_d means that the dust dominates the total particles.

The coarse dust backscatter coefficient β_{dc} is obtained by the following equation:

$$\beta_{dc} = \begin{cases} \beta_p & \delta_p \geq \delta_{dc} \\ \beta_p \frac{(\delta_p - \delta_{nd+df})(1+\delta_{dc})}{(\delta_{dc} - \delta_{nd+df})(1+\delta_p)} & \delta_{nd+df} < \delta_p < \delta_{dc} \\ 0 & \delta \leq \delta_{nd} \end{cases} \tag{S2}$$

Here, δ_{dc} is the coarse dust depolarization ratio and δ_{nd+df} is the depolarization ratio of mixture of non-dust and fine dust particles. δ_{df} and δ_{dc} are estimated to be 0.16±0.02 and 0.37±0.03, respectively under the wavelength of $532\,\mathrm{nm}$.

Figure S2 shows the depolarization ratio profiles in correspondence to the 4 cases in the manuscript. Values greater than 0.31 are assigned as red. By comparison with the extinction coefficient profiles, the depolarization ratio profiles show that the dust is the dominant particle in these 4 cases.

3. Vertical localization

The vertical localization is implemented by applying a correlation coefficient into the assimilation analysis process. The correlation coefficient decreases with the increase of altitude differences between ground and the specific layer. The function is denoted as:

$$c = exp(-3h^d) \tag{S3}$$

Here, c represents the correlation coefficient and h^d is the altitude difference. As the fig. S3 shows, c decreases rapidly when h^d increases. The most noticeable decreases occur in between 100 to 1000 m. The c decreases to 0.4 when $h^d = 300\,\mathrm{m}$.

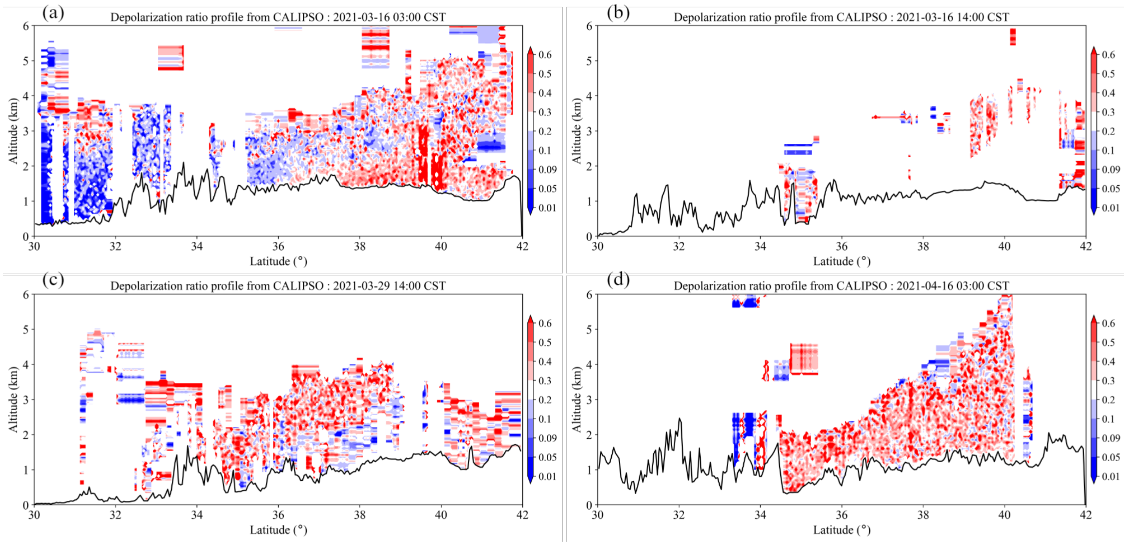

Fig. S2. Depolarization ratio profiles from CALIOP for the correspondent 4 cases.

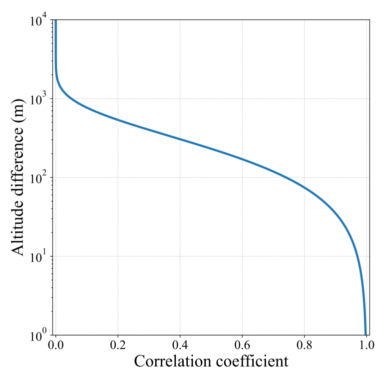

Fig. S3. Relation between correlation coefficient and altitude differences. The y axis is Logarithmized.

4. Impact of vertical localization

The vertical localization scheme is applied in the assimilation of case *P-Gd-CAL* and *N-Gd-CAL*. They are referred to as *P-Gd-CAL-L* and *N-Gd-CAL-L*, respectively. Figure S4 is the posterior profiles from these two cases. In the presence of correct vertical structure, through the comparison between fig. 3 (d.2) and fig. S4 (a), it can be found that concentrations on ground are close to each other while the upper concentrations are closer to prior in *P-Gd-CAL-L*. This is cased by the constrain of vertical localization scheme. By the comparison of altitudinal R (in fig. S5 (a)), it can be clearly noticed that R in *P-Gd-CAL-L* decreases with altitude and becomes in line with prior above the 2 km. However, *P-Gd-CAL* continue to show improvements above the 2km. In the presence of incorrect vertical structure, it can be noticed that although the incorrect upper concentrations are not inflated much (see comparison between fig. 4(d.2) and fig. S4 (b)), it shows no improvement compared to simple EnKF (in fig. S5 (b)).

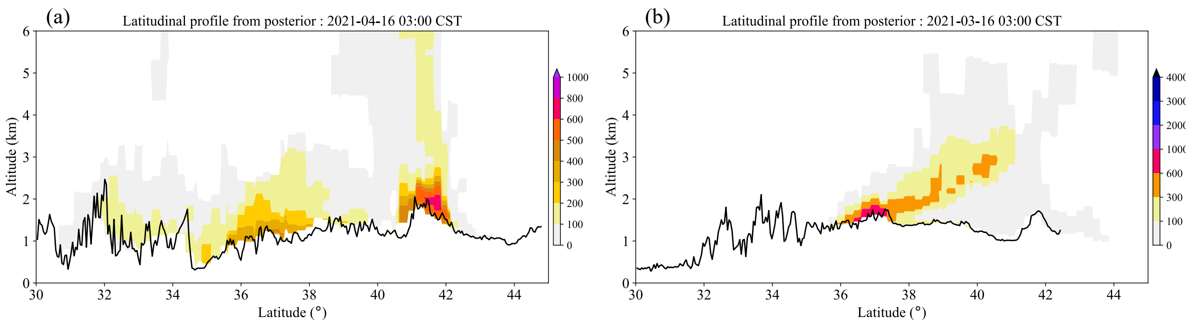

Fig. S4. Dust concentration profiles following the CALIPSO scanning trajectory from the posterior of *P-Gd-CAL-L* (**a**) and *N-Gd-CAL-L* (**b**).

5. Statistical evaluation

Figures S5 and S6 are the altitudinal and latitudinal trend of correlation coefficient (R) between concentration fields and CALIPSO observations. The fields are linear interpolated into the CALIPSO data point. These data are paired within the altitudinal and latitudinal direction. In the case of *P-Gd-CAL* and *N-Gd-CAL*, as shown in figs. S5 and S6 (a,b), it can be noticed that ground data assimilation can optimize the dust field under the correct vertical structure. Improvements of R can be seen in the 1st case. Meanwhile, as figs. S5 and S6 (b) shows, it can also maintain the incorrect vertical structure. In the case of DOD assimilation, similar trend is shown. The incorrect vertical structure remains after assimilation. Moreover, there is a noticeable degrade of R found in fig. S6 (c), which is in line with the inflated incorrect dust structure in *NP-DOD-CAL*.

References

1. Mamouri, R. E. and Ansmann, A.: Fine and Coarse Dust Separation with Polarization Lidar, Atmos. Meas. Tech., 7, 3717–3735, https://doi.org/10.5194/amt-7-3717-2014, 2014.
2. Mamouri, R.-E. and Ansmann, A.: Potential of Polarization/Raman Lidar to Separate Fine Dust, Coarse Dust, Maritime, and Anthropogenic Aerosol Profiles, Atmos. Meas. Tech., 10, 3403–3427, https://doi.org/10.5194/amt-10-3403-2017, 2017.

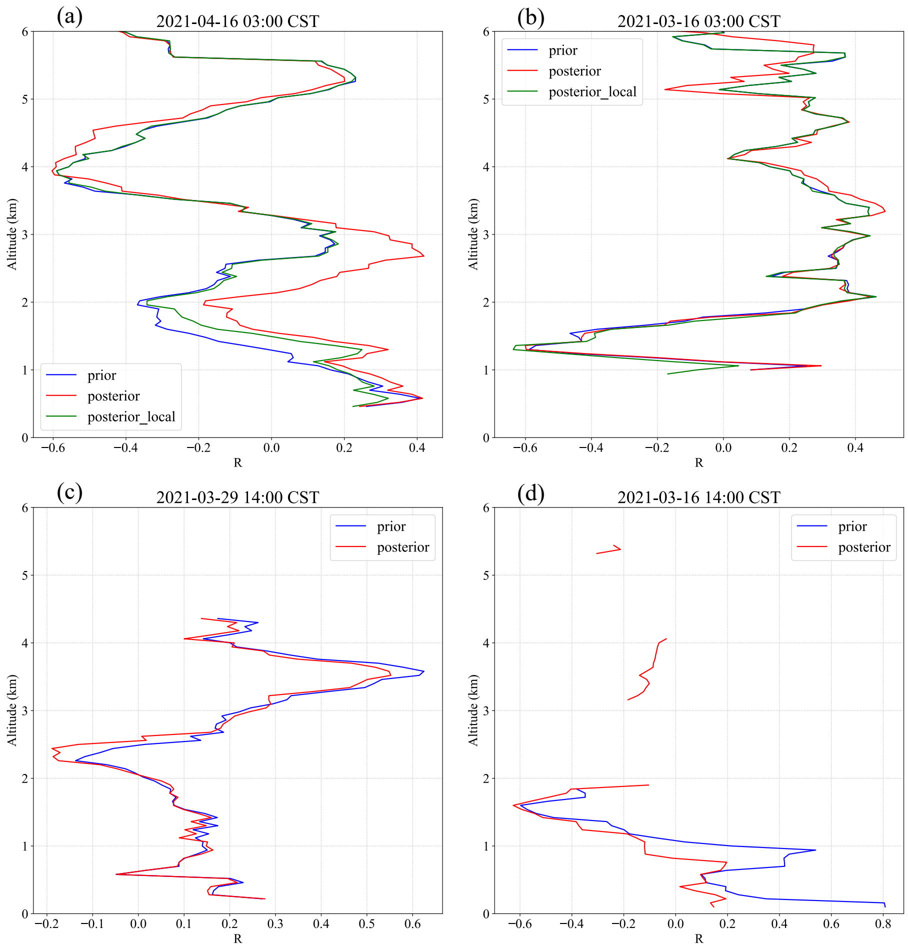

Fig. S5. The correlation coefficient averaged on different altitudes. Each altitude contains all the paired data points (Concentration and extinction coefficient) along with the CALIPSO scan line

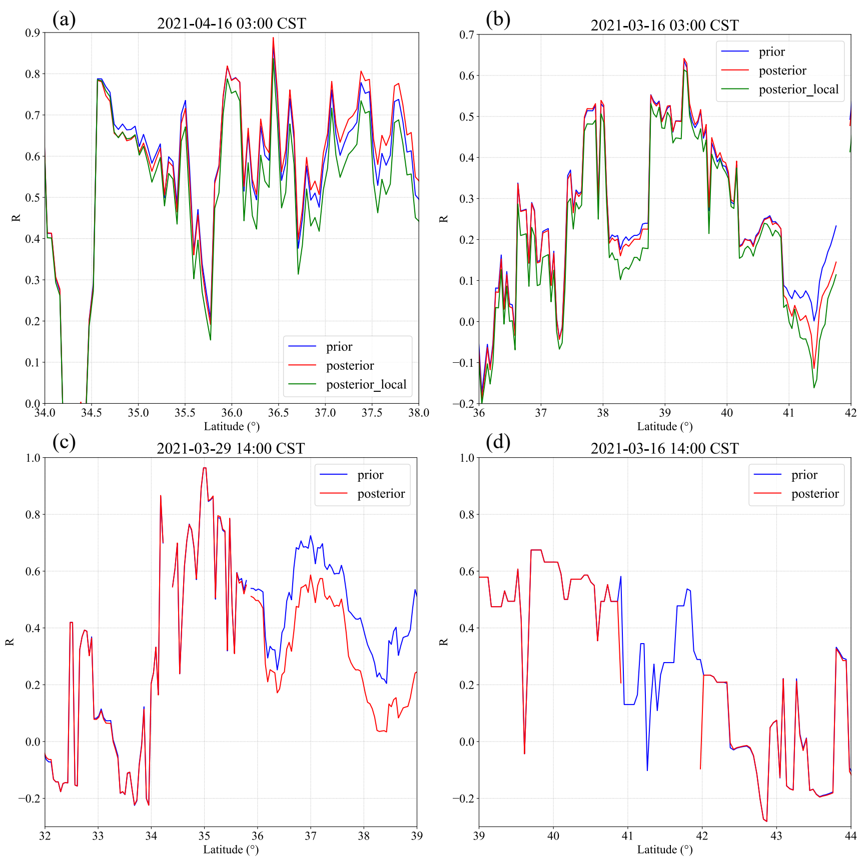

Fig. S6. The correlation coefficient averaged on different latitudes. Each latitude contains all the paired data points (Concentration and extinction coefficient) along with the CALIPSO scan line